ISSN 1392 - 1207. MECHANIKA. 2013 Volume 19(1): 25-32

Numerical investigation of the heat transfer in an annulus cylindrical space

A.Z. Dellil*, A. Azzi**
**Institute of maintenance and industrial safety, University of Oran; Laboratory of mechanics applied, USTO, Oran, Algeria, E-mail: sdellil@yahoo.fr*
***USTO, Oran, Algeria, E-mail: AbbesAzzi@yahoo.fr*

crossref http://dx.doi.org/10.5755/j01.mech.19.1.3613

Nomenclature

e - width of the magnetic gap, m; C_p - specific heat with constant pressure, J/Kg C°; h - coefficient of heat transfer by convection, w/m^{2}C°; K - kinetic energy turbulent; L - lenght of rotor, m; V - axial speed of fluid, m/s; w - angular velocity, rd/s; Nu - Nusselt Number; Pr - Prandtl Number; Ta - Taylor Number; $(Ta)_m$ - Taylor Number modified; r_e - interior radius of stator, m; r_i - exterior radius of rotor, m; λ - thermal conductivity, w/mC°; v - kinematic viscosity, m^2/s

1. Introduction

The design of electrical or electronic components, more and more miniaturized, high reliability is limited by other considerations, in particular for problems of heat dissipation. All electrical components, electrical, are sensitive to temperature, their performance decreases with increasing temperature. They can be destroyed under the effect of this temperature. The study of heat transfer phenomena in this type of electrical machinery has been the subject of much research. Found in these machines a combination of physical processes from electrical, mechanical and magnetic. The quantity of heat generated by irreversible phenomena resulting in high levels of temperature in parts of these machines (insulation, bearings). The evacuation of this heat requiring more or less bulky accessories is not always easy, especially in the field of aviation, where improving the specific power through the optimization of cooling the engine. Dissipations originate mainly in the electrical conductors and ground magnetic force of the rotor and stator. These two subsets of an electric machine [1] is called an annular magnetic gap which circulates a cooling fluid. Depending on the technology used, the fluid usually used, is the air that passes between the rotating rotor and the stator immobile. Our study therefore concerns ways to improve this transfer, because the energy dissipated in the resistance heating of a rotor-stator is not carried in its entirety by the airflow.

A part is lost by it by radiation of this wall towards the fluid and consequently towards the outer wall of the rotor. This energy is not negligible. Recent work shows the possibility of reinforcing in a spectacular way the heat transfers within the electric machines by the introduction of grooves, the flow of air in the air-gap resulting from the swing drive and the effect of work of a fan.

Fig. 1 shows that a weak increase in a few degrees of the operating temperature causes an exponential increase in the number of failures [2].

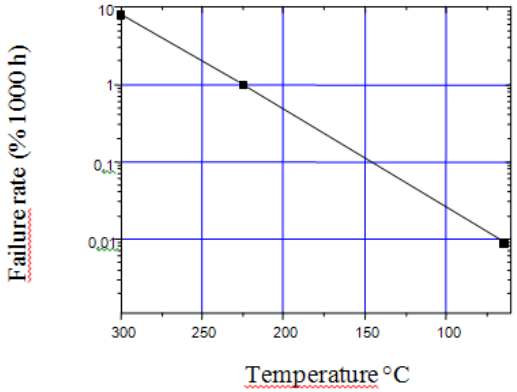

Fig. 1 Variation of the failure rate

The objective in this study is to show the impact of speed of rotation of the rotor, the axial velocity of air and especially the impact of the presence of the grooves of the rotor or stator. Studies have shown that there may be four flows in the annular space formed by a rotor moving in immobile stator:

- laminar flow;
- laminar flow with secondary flow (Taylor vortices);
- turbulent flow;
- Turbulent flow with Taylor vortices [3].

The impact of the change in geometry by the presence of grooves on either the rotor or the stator according to the variation in the speed of rotation of the rotor and the axial velocity of the cooling air will be the key our study. For this, we chose three main configurations: smooth pipe, grooved rotor, grooved stator. Initially, we studied the flow of air in to the smooth air magnetic gap for different rotor speed and for different axial velocities of air. In a second step, through the presence of flutes on either the rotor or the stator and with the same variables, we modeled the convective exchanges in this space. Various studies have been conducted on the annular spaces. The influence of variables that control heat transfer in the annulus of electrical machines such as:

- the speed of rotation of the rotor;
- the speed of axial air space;
- the temperature gradients in the magnetic gap;
- roughnesses of surface in this air-gap were carried out by Kaye and Elgar [4].

The complexity of the problem led the authors to retain only the first three alternatives. These authors point out the results of work of G. I. Taylor [3].

The latter studied the stability of an incompressible viscous flow in the magnetic gap formed by coaxial

cylinders of infinite length and rotation without axial flow. The main result of this analysis is the characterization of several types of flows depending on the number of Taylor. Above a certain value, we see the emergence of a secondary flow consisting of counter-rotating vortices. In this study the authors have maintained the ratio of the width of the magnetic gap in average radius constant. Other authors [5] continued the study of heat transfer for an axial flow without rotation and with rotation. They have introduced the concept of modified Taylor number that reflects the geometric shape factor. In addition to the results obtained by [5] and that are verified by Bjorklund and Kays [6] for different values of the ratio e/r_m. However, the results of Gazley [7] deviate from nearly 30% of those of other authors. Taking different cooling fluids for a variety of different speed and value of the magnetic gap, F. Tachibana [8] has focused on heat transfer in this space. He noted for low speed and low width of the magnetic gap, the drop in Nusselt number. Much of this heat is radiative in nature and thus explaining the low conductive heat transfer by convection. With increasing speed and the magnetic gap, the Taylor number increases thereby resulting the appearance of secondary flow. In this case, there's no radiation and conduction to convection. Aoki [9] introduced the concept of Taylor number modified by looking on heat transfer of magnetic gap for different values of speed and different fluids. Since the first work of Taylor [3], studying the stability of the flow and heat transfer phenomena in a smooth annular space, in the absence of axial flow, has been the subject of numerous studies both theoretical and experimental Di Prima and Swinney [10] and Maron and Cohen [11] have treated this subject. The main conclusion, that beyond a critical value of the speed of rotation of the vortex superimposed on the Couette flow significantly increase the transfers between the walls [9]. Gazley [12] was the first to look at a narrow magnetic gap arising from several different configurations of smooth or fluted walls of the rotor or stator. For corrugated annular spaces, there are few results [11]. By cons, in groove magnetic gap, Gardiner et al. [13] conducted their work using water as coolant. The speed can reach 6000 rpm for the rotor which corresponds to a value of Taylor number of 4.8×10^4. In the presence of axial flow, the flow is turbulent and characterized by Reynolds numbers up to values of 3.1×10^4 and 1.7×10^4 in clean configuration grooved configuration. An opening in the center of the stator has to Pellé and Harmand [14] experimentally show the improvement of heat transfer even locally.

2. Numerical model (SST)

To evaluate the thermal exchanges in the rotor-stator configuration, numerical simulations were carried out by the code CFX 11. For cooling the rotor-stator was used SST (Shear-Stress-Transport) (Menter [15]). Several authors have focused their work on the development of advanced turbulence. Among them, we notes work of Kraft et al. [15], Leschziner [16], Leschziner and Ince [17], Hanjalic [18]. This othors used the models of the second order. Many strategies have been developed recently to capture the maximum information near the wall (fineness of the mesh) and away from it (and Rodi model Scheuerer [20]). Seen the many deficiencies of these models, an alternative is to use a specific equation of dissipation (frequency and large eddy) developed by Wilcox [21]. One of the main advantages of this model is robust even for complex geometries. Compared to the standard model, Menter [15] showed that the main deficiency of the model is its high sensitivity for jets outside the boundary layer. To avoid this, a combination of the model, away from the wall and near wall model was developed and called SST.

2.1. Mathematical model

Thestandard modelis a modelthatisbasedon solvingthetransport equationsofturbulent kinetic energy *k*anditsdissipation rate ε.The flowisassumedfullyturbulentandtheeffects ofmolecular viscosityarenegligible.

Transportequationsfor themodel k - ε

$$\frac{\partial(\rho k)}{\partial t}+\frac{\partial(\rho U_j k)}{\partial x_j}=P_k-\rho\varepsilon+\frac{\partial}{\partial x_j}\left(\Gamma_k\frac{\partial k}{\partial x_j}\right); \quad (1)$$

$$\frac{\partial(\rho\varepsilon)}{\partial t}+\frac{\partial(\rho U_j \varepsilon)}{\partial x_j}=C_{\varepsilon1}\frac{\varepsilon}{k}P_k-C_{\varepsilon2}\rho\frac{\varepsilon^2}{k}+ +\frac{\partial}{\partial x_j}\left(\Gamma_\varepsilon\frac{\partial\varepsilon}{\partial x_j}\right), \quad (2)$$

with the constants:

$$C_{\varepsilon1};\ C_{\varepsilon2};\ \sigma_k;\ \sigma_\varepsilon;\ \Gamma_k=\mu+\frac{\mu_t}{\sigma_k};\ \Gamma_\varepsilon=\mu+\frac{\mu_t}{\sigma_\varepsilon}. \quad (3)$$

P_k represents production of turbulent kinetic energy due to the gradient of the average velocity:

$$P_k=\mu_t\left(\frac{\partial U_i}{\partial x_j}+\frac{\partial U_j}{\partial x_i}\right)\frac{\partial U_i}{\partial x_j}+\frac{2}{3}\rho k\delta_{ij}\frac{\partial U_i}{\partial x_j}. \quad (4)$$

μ_t is eddy viscosity is computed by combining k and ε:

$$\mu_t=C_\mu\rho\frac{k^2}{\varepsilon}, \quad (5)$$

where C_μ is a constant model. Reynolds tensors are calculated from the relation Boussines:

$$\rho\overline{u_i u_j}=-\mu_t\left(\frac{\partial U_i}{\partial x_j}+\frac{\partial U_j}{\partial x_i}\right)+\frac{2}{3}\rho k\delta_{ij}. \quad (6)$$

2.2. Model k-ω

The turbulent kinetic energy k and its specific rate of dissipation ω are obtained from the following equations:

$$\frac{\partial(\rho k)}{\partial t}+\frac{\partial(\rho U_j k)}{\partial x_j}=P_k-\beta'\rho k\omega+\frac{\partial}{\partial x_j}\left(\Gamma_k\frac{\partial k}{\partial x_j}\right). \quad (7)$$

The constants have values:

$$\beta'=0.09;\ \alpha=5/9;\ \beta=3/40;\ \sigma_k=2.0;\ \sigma_w=2.0. \quad (8)$$

2.3. Turbulence model SST

The SST model has demonstrated the potential for accurate predictions of separation in many cases. The idea behind the SST is to combine the model *k*-*ε* and the model *k*-*ω* with a damping coefficient f_1. f_1 is equal to 1 near the wall and zero far from it. It activates the model of Wilcox (*k*-*ω*) in the region near the wall and the model for the rest of the flow. The formulation of the model SST is as follows:

$$\frac{\partial(\rho k)}{\partial t}+\frac{\partial(\rho U_j k)}{\partial x_j}=\tilde{P}_k-\beta^*\rho k\omega+\frac{\partial}{\partial x_j}\left(\Gamma_k\frac{\partial k}{\partial x_j}\right); \quad (9)$$

$$\frac{\partial(\rho\omega)}{\partial t}+\frac{\partial(\rho U_j\omega)}{\partial x_j}=\frac{\gamma}{\nu_t}P_k-\beta\rho\omega^2+$$

$$+\frac{\partial}{\partial x_j}\left(\Gamma_\omega\frac{\partial\omega}{\partial x_j}\right)+2\rho\sigma_{\omega 2}\frac{1}{\omega}\frac{\partial k}{\partial x_j}\frac{\partial\omega}{\partial x_j}; \quad (10)$$

$$\Gamma_k=\mu+\frac{\mu_t}{\sigma_k};\ \Gamma_\omega=\mu+\frac{\mu_t}{\sigma_\omega};\ P_k=\tau_{ij}\frac{\partial U_i}{\partial x_j}; \quad (11)$$

$$\tilde{P}_k=min\left(P_k,C_{1\varepsilon}\right).$$

The coefficients φ_1 and φ_2 are the model functions:

$$\varphi=f_1\varphi_1+(1-f_1)\varphi_2, \quad (12)$$

where the model coefficients *k*-*ω* and the model *k*-*ε* are equal to: $\sigma_{k_1}=2.0$; $\sigma_{w_1}=2.0$; $\kappa=0.41$; $\gamma_1=0.5532$; $\beta_1=0.075$; $\beta^*=0.09$; $C_1=10$; $\sigma_{k_2}=2.0$; $\sigma_{w_2}=1.168$; $\gamma_2=0.4403$; $\beta_2=0.0828$.

2.4. Presentation of the CFX code

The ANSYS-CFX code is used in the simulation of the complex flow encountered in Turbomachinery, and of the heat transfer by convection in annulus-cylindrical space of an axial flow of air, between a rotor turning at constant angular velocity and a fixed stator. The ANSYS-CFX code is organized into different blocks linked to each other by the running of the problem data for a computational fluid dynamic analysis (CFD).

The ICEM CFD block has the function for preparing the geometrical configuration of the treated problem and generating the grid in very complex cases. It employs mono or multi-block structures depending on the geometry to handle and it is capable to generate tetrahedral and hexahedral grids.The CFX –Pre can read a lot of grids from a variety of sources. The CFX-Solver has the task of solving the modeling problem hydrodynamic equations.

2.5. The grid

The geometry is composed of 262196 elements and 236000 nodes for each case studied (Fig. 2).

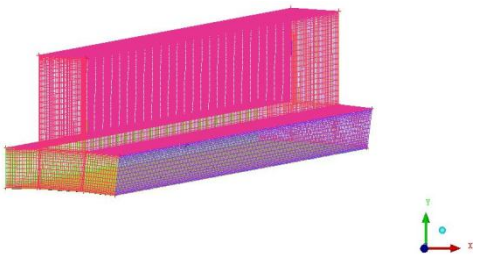

Fig. 2 Statorgrooved

2.5.1. Smooth tube

Driving without a corrugated, we tested several magnetic gaps, to evaluate the impact of space on the heat transfer. Heat transfer in this space called magnetic gap is influenced by the speed of rotation of the rotor, the speed of air blowing, the temperature gradient between the stator and rotor, the surface roughness. G. I. Taylor [3] by analyzing the stability of the viscous flow in this magnetic gap brought the Taylor number which characterizes this type of flow:

$$Ta=\frac{\omega^2 R_1\left(\frac{d_h}{2}\right)^3}{\nu^2}. \quad (13)$$

If this number is below a critical value, the flow is laminar. There is an appearance of counter-rotating vortex if you exceed this critical value.

2.5.2. Corrugated tube

The numerical study is conducted in an annulo-cylindrical geometry with a corrugated rotor and a corrugated stator. The model used is the SST. For this geometry fluted (corrugated rotor or stator) the Taylor number is modified taking into account the shape of the corrugated (form factor): *F* - geometric factor based on the work of [3]; *ω* - the speed of rotation, rd/s; *e* - thickness of the magnetic gap, m.

$$Nu=0.064T_{am}^{0.367}; \quad (14)$$

$$T_{am}=\frac{\omega^2 r_m}{\nu^2}\left(\frac{1}{F}\right); \quad (15)$$

$$r_m=\frac{e}{\ln R_2/R_1}\ \text{with}\ F=\frac{\pi^4}{1697}\left[1-\frac{e}{2r_m}\right]^{-2}p^{-1}; \quad (16)$$

$$P=0.0571\left[1-0.652\left(\frac{e/r_m}{1-e/r_m}\right)\right]+$$

$$+0.00056\left[1-0.652\left(\frac{e/r_m}{1-e/r_m}\right)\right]^{-1}. \quad (17)$$

For different axial and tangential velocities, we introduce the different Reynolds numbers:

$$R_{eaxial}=Vd_h/\nu \quad (18)$$

and

$$R_{etangentiel} = \omega R_1 d_h / \nu. \quad (19)$$

Speeds of the air flow in the air-gap: v = 1 , 3 and 8 m/s.

2.5.3. Boundary conditions

- The input surface defined as entrance surface;
- the flow regime is subsonic;
- the intensity of turbulence is taken equal to 5%
- the normal speed of the airflow to the entry varies from 1 to 8 m/s.
- the temperature of the air is taken equal to 25°C.
- the gradient of pressure at the exit is equal to 0
- the outer surface of the wall defined as a solid wall with a constant temperature of 93°C for the stator;
- for the moving rotor, the wall is raised to 204°C and rotating at different speeds ranging from 2.7 to 620 rd/s.

We adopted a refined mesh in 0 grid.

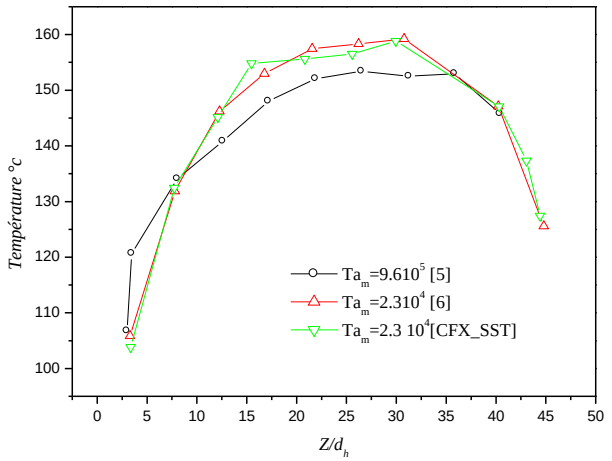

Fig. 3 Evolution of temperature along the cylindrical pipe

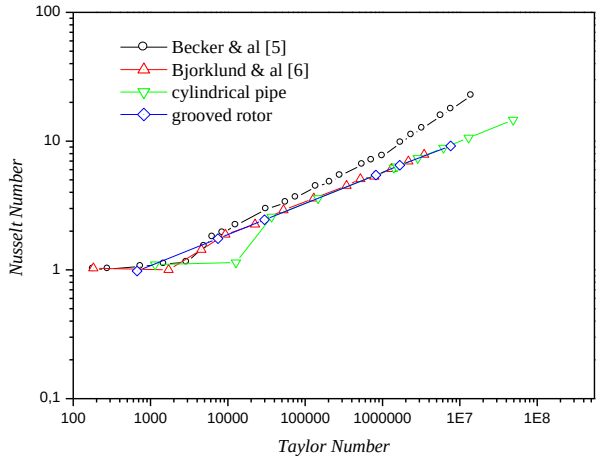

Fig. 4 Evolution of the Nusselt number based on the number of Taylor

We have confirmed our study by comparing governing numerical results with those obtained by [6]. The model selected was used to follow the shape of temperature profile. The corresponding curve (Fig. 3) at selected grid is super imposed on the experimental curve [6]. The evolution of Nusselt number follows the same profile as of Bjorklund [6] for various rotational speeds and axial velocities of the fluid cooling the rotor-stator (Fig. 4).

2.6. Validation of results

To validate our numerical work, we tested three grids (Table), the grid structure consists of 262196 elements.

Table

Grids tested

	Type	Elements	Nodes
Mesh 1	hexahedral	431034	411000
Mesh 2	hexahedral	276000	245916
Mesh 3	hexahedral	262196	236000

3. Results

3.1. Smooth pipe

It is observed for the same axial velocity of air, the temperature evolution takes the same shape along the rotor, whatever speed and whatever the value of the magnetic gap.

3.1.1. Impact the value of the magnetic gap

For large values of the magnetic gap, convection prevails before the conduction and little radiation surfaces because there has viscous dissipation of fluid in the magnetic gap. For low value of the gap (Fig. 5), we note that most of the transfer of heat is transferred by conduction. In this case, the conduction to convection prevails in this small space where the fall of the Nusselt number. There is a discontinuity in the shape of the curve for low values of the magnetic gap.

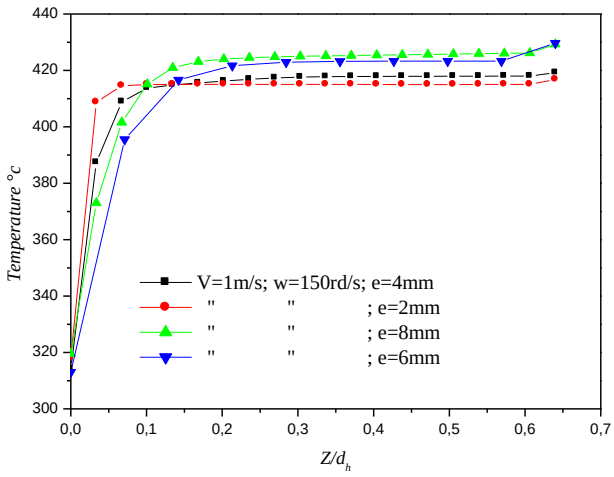

Fig. 5 Impactof the magnetic gap: V = 1 m/s, w = 150 rd/s

This discontinuity reflects a passage from an area governed by the laws of the laminar flow to an area where the flow is turbulent. In fact, Fig. 5 shows the evolution of temperature for different values of the magnetic gap. The profile is linear from along the smooth pipe for all values of the magnetic gap. However, the difference is not important for low values of this magnetic gap. we note on the above figure, an increase of temperature around 10°C for a

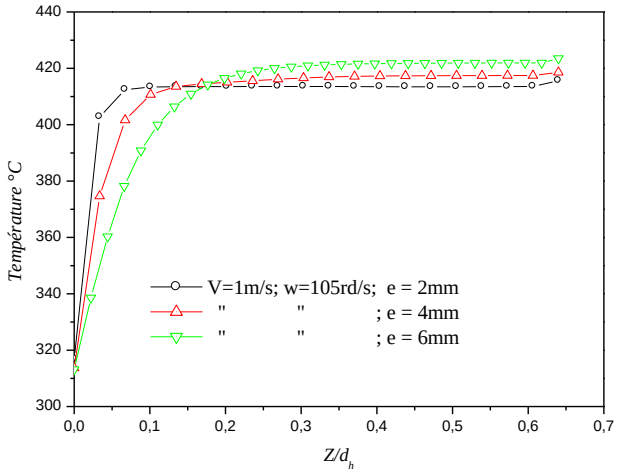

Fig. 6 Impactof the magnetic gap: V = 1 m/s, w = 105 rd/s

magnetic gap e = 8 m

We observe in this Fig 6 that the evolution for both profiles is the same, but a difference of 20°C is present when the rotational speed increases from the value of 3 rd/s to 150 rd /s and the gap varies from 2 mm to 6 mm. By increasing both variables, the speed of rotation of the rotor and the value of the magnetic gap, we obtain an increase in the heat transfer in the range of 5%. In this case, the majority of the transfer is by convection, in addition to the Taylor number is proportional to the square of the speed of rotation causes the appearance of a secondary flow.

3.1.2. Impact of speed

It can be seen in Fig. 7 and 10, all temperature profiles show a linear profile along the rotor (for Z / dh varying from 0.2 to 0.6). The impact of speed of rotation is clearly visible from 3 rd/s up 320 rd/s. The temperature

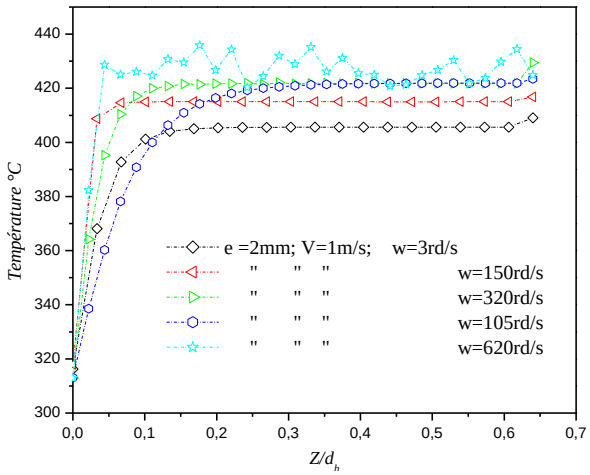

Fig. 7 Impact of rotational speed for a magnetic gap, e = 2mm

increases with speed. The difference is visible in the temperature profile, we note for example in this Figs. a gain of about 20°C, which is not negligible. By against when switching to 620 rd/s, the temperature profile is more linear.

It can be seen in Fig. 8, a difference of 40°C between the linear profile of temperature at low speed (3 rd/s) and high-speed 320 rd/s. We confirmed this

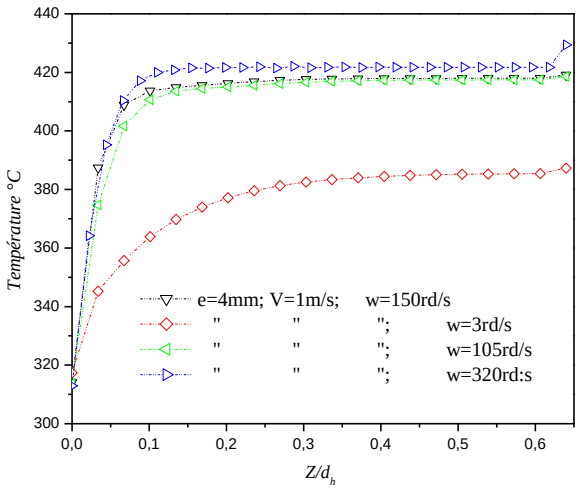

Fig. 8 Impact ofrotational speedfora magnetic gap, e = 4 mm

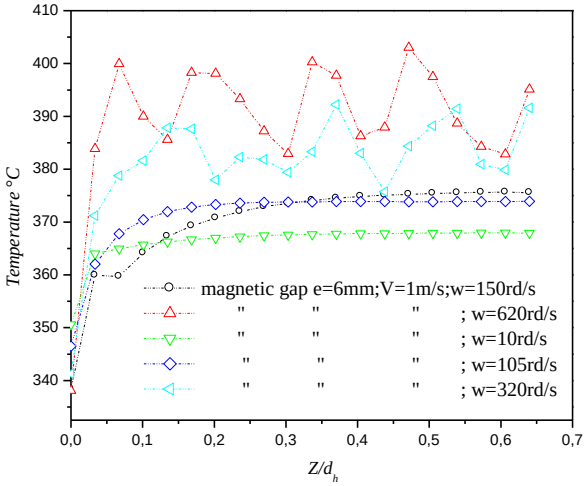

Fig. 9 Impact of rotational speed for a magnetic gap, e = 6 mm

through the Fig. 9 (e = 6 mm), because the temperature difference is accentuated when the rotor turns at high speed (620 rd/s).

For the value of the magnetic gap equal to 6 mm and beyond the latter, the temperature profiles become non linear for high speeds of rotation. Hence the choice of a value of the magnetic gap not exceeding 6mm. Finally, we observe that the impact of speed of rotation is found along the pipe.

3.2. Corrugated pipe

3.2.1. Rotor and stator corrugated

After pipe smooth, and at first we modelled the rotor corrugated, then the stator corrugated with the same mesh. The overall results for these two cases confirm the results of smooth driving. Fig. 10 shows the temperature distribution for the grooves of the rotor heated. We Note the presence of counter-rotating vortices inside each groove grooved stator (Fig. 11). We have plotted in Figs. 12 and 13 the velocity profile, temperature and the kinetic energy for different air speed and different speeds of rotation. We notice the same behaviour changes for the stator and rotor corrugated.

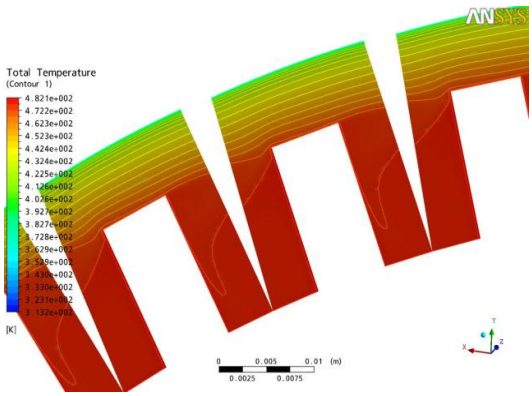

Fig. 10 Rotor temperature contour grooved

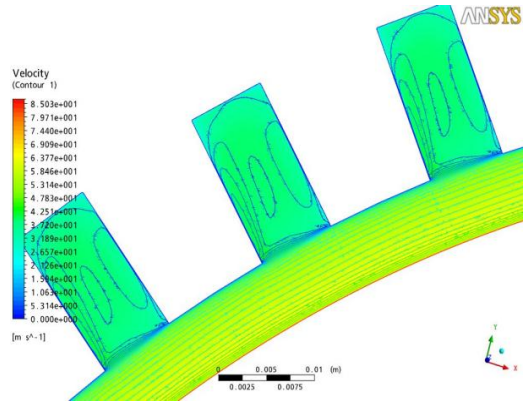

Fig. 11 Contour speed grooved stator

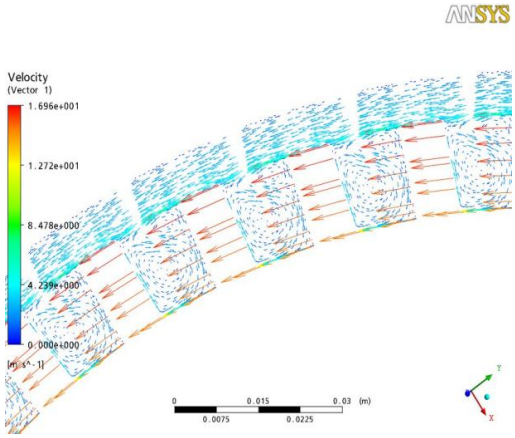

Fig. 12 Velocity distribution inside the grooves (grooved rotor)

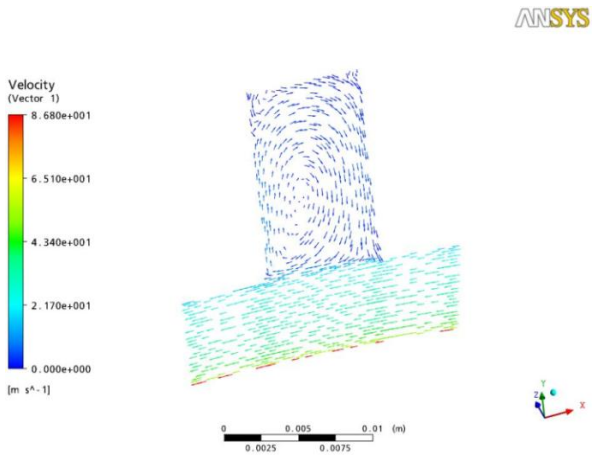

Fig. 13 Velocity distribution inside thegrooves (grooved stator)

On the following Figs. 15 and 16, we plot the evolution of the Nusselt number based on the number of Taylor. The transfer of heat through the Nusselt number is inflenced by the speed of rotation of the rotor (represented by the Taylor number). We observe in this Figs. 15 and 16, the dependence of Nusselt number with rotational speed speed for the rotor and the rotor corrugated smooth. The

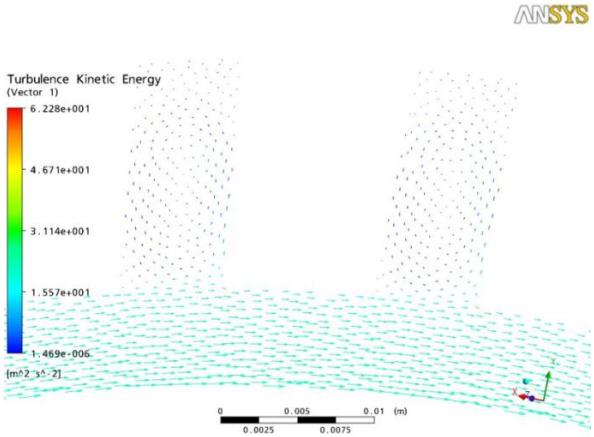

Fig. 14 Contour of the kinetic energy of the stator grooved

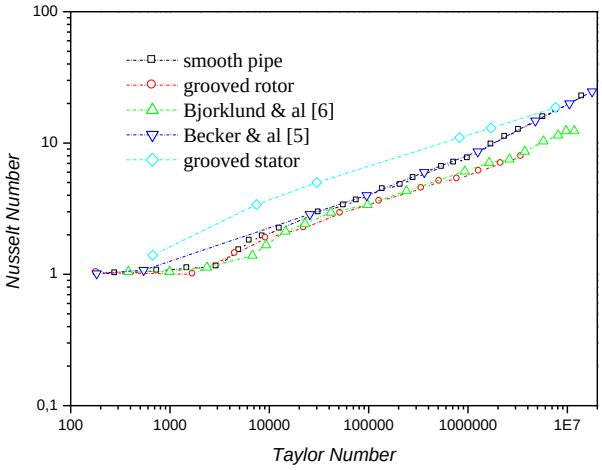

Fig. 15 Impact of rotational speed of the rotor on the Nusselt Number

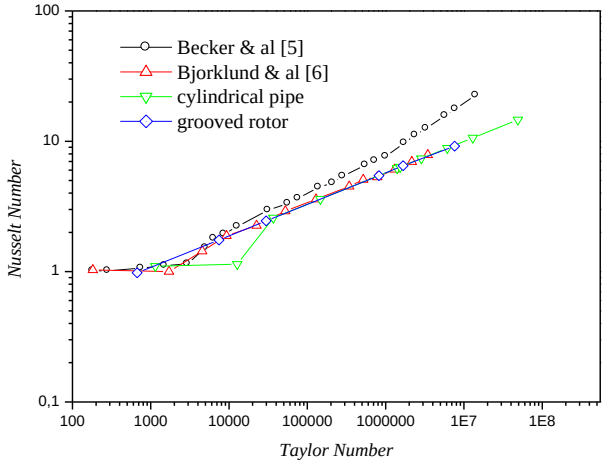

Fig. 16 Comparison between the cylindrical pipe, grooved rotor and stator grooved

shape of the Nusselt number for smooth pipe and corrugated rotor is similar to those obtained experimentally. There

is some discrepancy in the case of corrugated stator. We observe in this Fig. 14 the energy contribution for high speeds. The results are consistent with those of [5, 6] for different values of magnetic gap and speed of rotation. On the other hand, we note that those obtained by the stator corrugated deviate by about 20% of other authors.

3.2.3. Comparison between the rotor and stator corrugated

We plot the following Figs. 17-19 the evolution of Nusselt number along the pipe smooth or corrugated. Whatever the speed and air flow, the evolution of Nusselt number is constant and depends on temperature gradient imposed between the walls. However, we note that for all

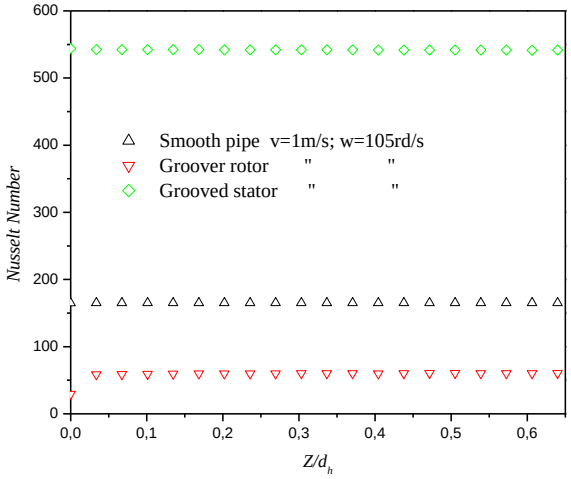

Fig. 17 Comparison of Nusselt number for the three cases (V = 1 m/s, w = 105 rd/s)

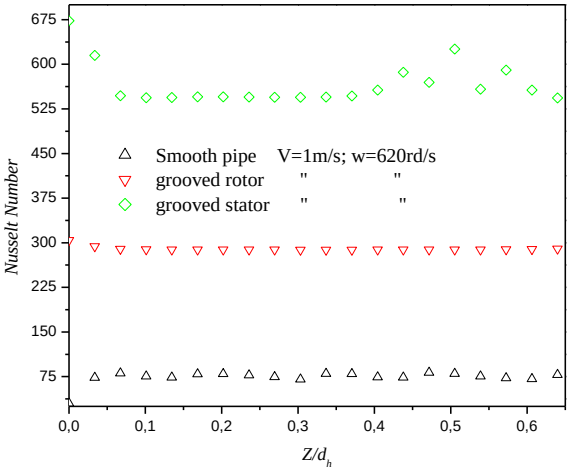

Fig. 18 Comparison of Nusselt number for the 3 cases (V = 1 m/s, w = 620 rd/s)

cases, the Nusselt grooved stator is high and is around 200 to 300. Its value is twice that of the rotor and corrugate triple compared to the smooth pipe. For the same rotational speed of therotor, there isthe same profile of the Nusselt number for the stator and rotor corrugated. If we compare the Nusselt number for three cases, namely the profile of Nusselt conduct smooth, grooved rotor and stator grooved; we see that the Nusselt is high compared to the other two speeds. With the high speed rotation, the Nusselt profile has not the same shape as the other speeds. Of all the above Figs. 17-19, we note the high dependence of Nusselt number opposite the rotational speed.

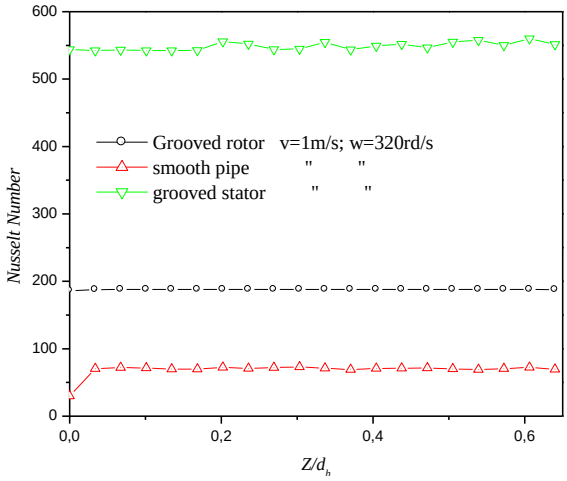

Fig. 19 Comparison of Nusselt number for the 3 cases (V = 1 m/s, w = 320 rd/s)

4. Conclusion

We studied numerically the convective transfer in turbulent flow for the three cases of figures. It follows from the numerical study results indicate that the dependence of the value of the magnetic gap and the speed of rotation of the rotor on the heat transfer especially for Taylor numbers than 1700.

We observed on the configuration of the rotor smoothes the increase in the heat transfer when the number of revolutions and the value of the air-gap increase. Beyond 6 mm, the temperature profile is nonlinear (no influence of these parameters on the level of heat transfer). For the corrugated rotor and stator corrugated, we find the same looks and the same remarks. In turbulent flow, the model SST is the nature of this phenomenon. The comparison of numerical results with experimental results shows a satisfactory agreement using the SST model. In perspective, it remains to influence the nature of the cooling fluid, test other numerical models with other geometries.

References

1. **Ousten, J.P.; Khatir, Z.** 2011**.** Investigations of thermal interfaces aging under thermal cycling conditions for power electronics applications, Microelectronics Reliability, vol.51: 1830-1835. http://dx.doi.org/10.1016/j.microrel.2011.07.066.
2. **Cohen, M.G.; Chu, R.C.; Seely, J.H.** 1968. Thermal considerations and techniques for electronic circuit packaging in modern digital, computer, International electron circuit packaging symposium, session5/3, San Fransisco USA, 1-9.
3. **Taylor, G.I.** 1923. Stability of viscous fluid between two rotating cylinders, PhilTrans. R. Soc. London, Series A, 223: 289-343.
4. **Kaye, J.; Elgar, E.C.** 1958. Modes of adiabatic and diabatic fluid flow in an annulus with an inner rotating cylinder, Transactions of the ASME, 753-765.
5. **Becker, K.M.; Kaye, J**. 1962. Measurements of adiabatic and diabatic fluid flow in an annulus with an inner rotating cylinder, Journal of Heat Transfer, 84: 97-105. http://dx.doi.org/10.1115/1.3684335.
6. **Bjorklund, I.S.; Kays, W.M.** 1959. Heat transfer between concentric rotating cylinders, Journal of Heat

Transfer, 80: 79-90.
7. **Gazley, C.** 1958. Heat transfer characteristics of the rotational and axial flow between concentric cylinders, Journal of Heat Transfer, 80: 79-90.
8. **Tachibana, F.; Fukui, S.** 1964. Convective heat transfer of the rotational and axial flow between two concentric cylinders, bulletin of JSME, 7(26).
9. **Aoki, H.; Nohira, H.; Arai, H.** 1967. Convective heat transfer in an annulus with an Inner rotating cylinder, bulletin of JSME, 10(39): 523-532.
10. **Di Prima, R.C.; Swinney, H.L.** 1985. Instabilities and transition in flow between concentric rotating cylinders In Hydrodynamic Instabilities and Me Transition to Turbulence, ed. H.L. Swinney and J.P. Gollub, Springer, Berlin, 139-180.
11. **Maron, D.M.; Cohen, S.** 1991. Hydrodynamics and heat/ mass transfer near rotating surfaces, In Advances in Heat Transfer, Vol. 21, ed. T. F. Irvine and J.P. Harnett, Academic Press, New York, 141-183.
12. **Gazley, C.** 1977. Heat transfer characteristics of the rotationnel and axial flow between concentric cylinders, Journal of Heat Transfer, 99: 79-90.
13. **Gardiner, S.R.M.; Sabersky, R.H.** 1978. Heat transfer in an annular gap, International Journal of Heat and Mass Transfer, 21: 1459-1466. http://dx.doi.org/10.1016/0017-9310(78)90002-9.
14. **Pellé, J.; Harmand, S.** 2010. Echanges convectifs dans un systeme rotor-stator: Influence d'une ouverture au centre du stator, SFT, 53-58.
15. **Menter, F.R.** 1994. Two-equation eddy-viscosity turbulence models for engineering applications, AIAA-Journal, 32(8): 1598-1605. http://dx.doi.org/10.2514/3.12149.
16. **Craft, T.J. Launder, B.E.; Suga, K.** 1996. Development and application of a cubic eddy viscosity model of turbulence, Int. J. Heat and Fluid Flow, 17: 108-115. http://dx.doi.org/10.1016/0142-727X(95)00079-6.
17. **Leschziner, M.A.; Rodi, W.** 1981. Calculation of annular and twin parallel jets using various discretisation schemes and turbulence model variants, ASME J. Fluids Eng. 103: 352-360. http://dx.doi.org/10.1115/1.3241745.
18. **Inze, N.Z.; Leschziner, M.A.** 1990. Engineering turbulence modelling and experiments, Eds. W. Rodi and E.N. Ganic, Elseiver, 155-164.
19. **Hanjalic, K.** 1994. Advanced turbulence closure models: A view of current status and future prospects, Int. J. Heat Fluid Flow 15(3): 178-203. http://dx.doi.org/10.1016/0142-727X(94)90038-8.
20. **Rodi, W.; Scheuerer, G.** 1986. Scrutinizing the k–ε turbulence model under adverse pressure gradient conditions, ASME J. Fluids Eng. 108(2): 174-179. http://dx.doi.org/10.1115/1.3242559.
21. **Wilcox, D.C.** 1993. Turbulence Modeling for CFD, DCW Industries, Inc., La Canada CA.

A. Z. Dellil, A. Azzi

ŠILUMOS PERDAVIMO ŽIEDINIAME CILINDRE SKAITINĖ ANALIZĖ

R e z i u m ė

Šiame darbe pateikti šilumos mainų žiedinėje-cilindrinėje erdvėje tarp pastoviu greičiu besisukančio rotoriaus ir nejudančio statoriaus skaitinės analizės rezultatai, gauti esant išilginiam oro srautui. Analizuojami trijų geometrinių konfigūracijų atvejai. Pirmiausia laikoma, kad rotoriaus ir statoriaus paviršiai yra glotnūs. Antruoju atveju rotoriaus sienelė yra su grioveliais išilgai cilindro, o statoriaus glotni. Trečiuoju atveju statoriuje yra suformuoti tokie pat grioveliai. Skaitiniai rezultatai, gauti esant besisukančiam srautui (skirtingiems rotoriaus sukimosi greičiams), parodė, kad grioveliai skatina šilumos mainus didėjant sukimosi greičiui. Esant išilginiam oro srautui, turbulentinio tekėjimo rezultatai rodo, kad glotnus magnetinis tarpelis yra svarbus šilumos mainams. Ši skaitinė analizė atlikta naudojant CFX.11 kodą ir yra pagrįsta turbulentinio modelio taikymu: ŠĮP (šlytimi–įtempiais–pernešimu) įvertintas šilumos perdavimas rotoriaus ir statoriaus paviršiams.

A. Z. Dellil, A. Azzi

NUMERICAL INVESTIGATION OF THE TRANSFER HEAT IN AN ANNULUS CYLINDRICAL SPACE

S u m ma r y

This work concerns the numerical study of the transfer of heat by convection in annulus-cylindrical space of an axial flow of air, between a rotor turning at constant angular velocity and a fixed stator. Three cases of geometric configurations are studied. Initially, the surfaces of the rotor-stator are smooth. In a second step, the rotor wall is corrugated along the cylinder and the other is smooth and the last case is to achieve the same grooves on the stator. The numerical results obtained in rotating flow (for different rotation speed of the rotor) showed that the presence of the grooves increases the heat transfer as the speed increases. In the presence of an axial air flow, the results conducted in turbulent show that the case of smooth magnetic gap is interesting in terms of heat. This numerical study is performed with the code CFX.11 and based on the use of a turbulence model: SST (Shear-Stress-Transport) to evaluate the heat transfer in the Rotor-stator configuration.

Keywords: Cooling of the rotor-stator, modelling of turbulence, heat transfer.

Received June 25, 2011
Accepted December 19, 2012